

Channel Capacity Enhancement of SWIPT based CNOMA Downlink Transmission with Orbital Angular Momentum over Rician Fading Channel

Ahmed Al Amin · Soo Young Shin ·
Bhaskara Narottama

Abstract In this paper, orbital angular momentum (OAM) is integrated with power splitting based simultaneous wireless information and power transfer (SWIPT-PS) and cooperative non-orthogonal multiple access (CNOMA-SWIPT-PS) downlink transmission, called as CNOMA-SWIPT-PS-OAM. The proposed CNOMA-SWIPT-PS-OAM scheme enhances the spectral efficiency and energy efficiency as well. The SWIPT-PS will energize the relaying operation from cell center user (CCU) to cell edge user (CEU). Different symbols are transmitting towards the users simultaneously from the base station by utilizing different OAM modes on the time slot of relaying (CCU to CEU) for CNOMA-SWIPT-PS. The CCU, CEU and sum capacities and energy efficiency of the proposed scheme over Rician fading channels are investigated in this paper. Finally, the effectiveness of the proposed schemes over existing schemes and conventional orthogonal multiple access based scheme are demonstrated through the result analysis.

Keywords Cooperative non-orthogonal multiple access, · sum capacity, · energy efficiency, · orbital angular momentum · power splitting, · simultaneous wireless information and power transfer, · time switching

A.A. Amin
Department of IT Convergence Engineering, Kumoh National Institute of Technology, Gumi,
South Korea
E-mail: amin@kumoh.ac.kr

S. Y. Shin
Department of IT Convergence Engineering, Kumoh National Institute of Technology, Gumi,
South Korea
E-mail: wdragon@kumoh.ac.kr

B. Narottama
Department of IT Convergence Engineering, Kumoh National Institute of Technology, Gumi,
South Korea
E-mail: bhaskaranarottama@gmail.co

1 Introduction

Spectral efficiency along with energy efficiency (EE) are two vital challenges that need to be satisfied among the several requirements to achieve the upcoming challenges of the future wireless networks [1,2]. To deal with these challenges non-orthogonal multiple access (NOMA) and simultaneous wireless information and power transfer (SWIPT) can be integrated. Moreover, by utilizing the different modes of orbital angular momentum (OAM), additional symbols can be transferred to cell center user (CCU) and cell edge user (CEU) to enhance the channel capacities as well. These are the main focus of this paper.

NOMA is an interesting and suitable solution to enhance spectral efficiency and serve a large number of users [3,4]. In NOMA based system, the users are served simultaneously by the same code at the same frequency, time but different power levels. Successive Interference Cancellation (SIC) is used at the received end to separate the superimposed messages transmitted by the source [5].

Cooperative relaying is an effective way to enhance the reliability and coverage area by utilizing CCU as a relay for the CEU or using a dedicated relay which assists the NOMA users [6-9]. In general, the user closer from the base station (BS) is called CCU and the user further from BS is called CEU. NOMA with cooperative relaying is known as cooperative NOMA (CNOMA) [7-9].

Furthermore, RF signals can be utilized to energize the energy-constrained nodes. [10-11] This will enhance the battery lifetime by utilizing the SWIPT technique [12]. SWIPT, which can extract energy and information simultaneously from the ambient RF signals using power splitting or time switching receiver architecture, can provide RF energy harvesting (EH) at the energy-constrained nodes [13].

In present research work, CNOMA and SWIPT are integrated together which is known as CNOMA-SWIPT to provide spectral efficiency and energy efficiency as well [14-15]. CNOMA-SWIPT protocol can be categorized into two different types. In the first type, the CCU which is an energy-constrained node is used as a relay for the CEU [15-18]. In the second type, energy harvesting is used for the dedicated relay which relaying information for all NOMA users. The first type of CNOMA-SWIPT is the main consideration of this paper since dedicated relay is not available in every cases [19-20]. In the previous works, the ergodic sum capacity and outage probabilities are analyzed for the CNOMA-SWIPT protocol [21-22]. In the work of Kader et. al. [22], two novel cooperative spectrum sharing protocols, i.e., time switching (TS) and power splitting (PS), were investigated for CNOMA-SWIPT, where dedicated relay is used as an energy-constrained relay for the CEU. The ergodic sum capacity (ESC) and outage probabilities (OP) are analyzed for the CNOMA-SWIPT over Nakagami-m fading channel. In the work of Shah et. al. [23], a CNOMA-SWIPT protocol was proposed over Rayleigh fading channels. Whereas the source is communicating with the user with a backscattering node and an EH based decode and forwards (DF) relay technique. Moreover, in [24], a trans-

mit antenna selection scheme based on CNOMA-hybrid SWIPT protocol was proposed over the Rayleigh fading channel as well. Furthermore, the source is communicating with two users simultaneously via the support of an EH based decode and forwards (DF) relay technique. Furthermore, R. Jiao et. al. analyze the capacity of CNOMA over the Rician fading channel. However, the capacity enhancement and empowering the relaying node to enhance the energy efficiency are not analyzed to fulfill the requirements of the upcoming cellular communication system [25].

Considering all the above techniques, a suitable solution is required to energize the relay operation and provides enhanced channel capacity simultaneously without any additional resources. That is why CNOMA downlink transmission with PS based SWIPT protocol (CNOMA-SWIPT-PS) is a viable solution for simplicity and provides better capacities than TS as well [22]. So, CNOMA-SWIPT-PS is considered in this paper to energize the relay operation. OAM utilizes a new degree of freedom which is known as OAM mode for signal transmission [26-27]. Moreover, OAM exploits the phase variation with respect to the azimuth angle of the propagated electromagnetic waves. To enhance the capacity of CNOMA-SWIPT-PS, OAM is a potential candidate to transmit different symbols by utilizing different modes of OAM simultaneously to enhance the channel capacities without any interference [26-28]. That is why a novel scheme is proposed here by utilizing the time slot of relaying in the case of CNOMA-SWIPT-PS protocol. Two different additional symbols will be transmitted by different OAM modes towards the users from the base station (BS) by utilizing the same time slot for relaying from CCU to CEU. This proposed scheme can enhance the capacity of the CNOMA with PS SWIPT protocol without any interference and this scheme does not any required additional resources (e.g. time slot or frequency band) as well. Moreover, energy efficiency (EE) will be also enhanced by utilizing the proposed technique as well. The principal contribution of this paper is given below:

- PS based CNOMA-SWIPT-PS is considered over the Rician fading channel.
- OAM is integrated with CNOMA-SWIPT-PS protocol to achieve higher channel capacities. The proposed scheme of OAM with CNOMA-SWIPT-PS is mentioned as CNOMA-SWIPT-PS-OAM in this paper.
- To analyze the capacity enhancement of the proposed CNOMA-SWIPT-PS-OAM scheme, capacity of CCU, the capacity of CEU, and sum capacity (SC) are analyzed and investigated. Moreover, the capacities of the proposed scheme are compared with CNOMA based conventional SWIPT protocols (CNOMA-SWIPT-PS and CNOMA-SWIPT-TS) and conventional orthogonal multiple access (OMA) based SWIPT-PS with OAM (OMA-SWIPT-PS-OAM) as well.
- EE is another performance analysis metric that is analyzed here as well. Hence the EE comparison for the proposed scheme is compared with CNOMA and OMA based conventional SWIPT protocols as well.

- The impact of the different parameters over capacities and EE for the proposed scheme is analyzed and compared with CNOMA-SWIPT-PS, CNOMA-SWIPT-TS, and OMA-SWIPT-PS-OAM as well to analyze the effectiveness of the proposed scheme.

The rest of this paper is organized as follows. Section 2 describes the proposed CNOMA-SWIPT-PS-OAM system model and the proposed protocol as well. The capacity analysis and OMA based SWIPT-PS scheme are also presented in this section. Section 3 exhibits numerical results. This paper is concluded in Section 4.

2 System Model

A two-phase CNOMA-SWIPT-PS network with a BS which is considered as a source and two users (a CCU and a CEU) is considered. The BS directly communicates with the CCU called UE_1 and CEU called UE_2 as well. There is two line of sight (LOS) links that are considered from BS to UE_1 and UE_2 accordingly to send additional symbols directly to the users as well by different OAM modes. To enhance the data reliability at UE_2 and enhance the coverage area, UE_1 perform the energy harvested based decode and forward (DF) relaying from UE_1 to UE_2 . The proposed network model is shown in Figure 1. Hereafter, subscript s , 1 and 2 denote BS, UE_1 and UE_2 respectively. Assume that the channel coefficient $h_{p,q}$ between any two nodes p and q ($p, q \in \{s, UE_1, UE_2\}$ and $i \neq j$) is subjected to Rician fading plus Additive White Gaussian Noise (AWGN). Whereas, $\Omega_{s,1}$, $\Omega_{s,2}$, and $\Omega_{1,2}$ are the average power of BS to UE_1 , BS to UE_2 , and UE_1 to UE_2 relay link respectively, where $\Omega_{s,2} < \Omega_{s,1}$ [25]. The total transmits power of S for direct transmissions (NOMA and OAM) and power transmit from UE_1 for relaying are denoted by P and P_1 respectively. Moreover, $l_{s,1}$ and $l_{s,2}$ are two different OAM modes as well to transmit additional symbols to UE_1 and UE_2 respectively from the BS to enhance the capacities. The data communication policy along with the signal-to-interference-plus-noise ratio (SINR) model of the proposed CNOMA-SWIPT-PS-OAM scheme are discussed explicitly in section 2.1 and 2.2, respectively.

2.1 CNOMA-SWIPT-PS-OAM

In this strategy, it is considered that UE_1 acts as a PS based EH relay. Moreover, additional symbols are transmitted to the users as well by utilizing different OAM modes. The proposed system model and protocol summary are presented in Figure 1 and Figure 2 respectively. T is the total duration of downlink transmission of the CNOMA-SWIPT-PS-OAM scheme which is shown in Figure 2.

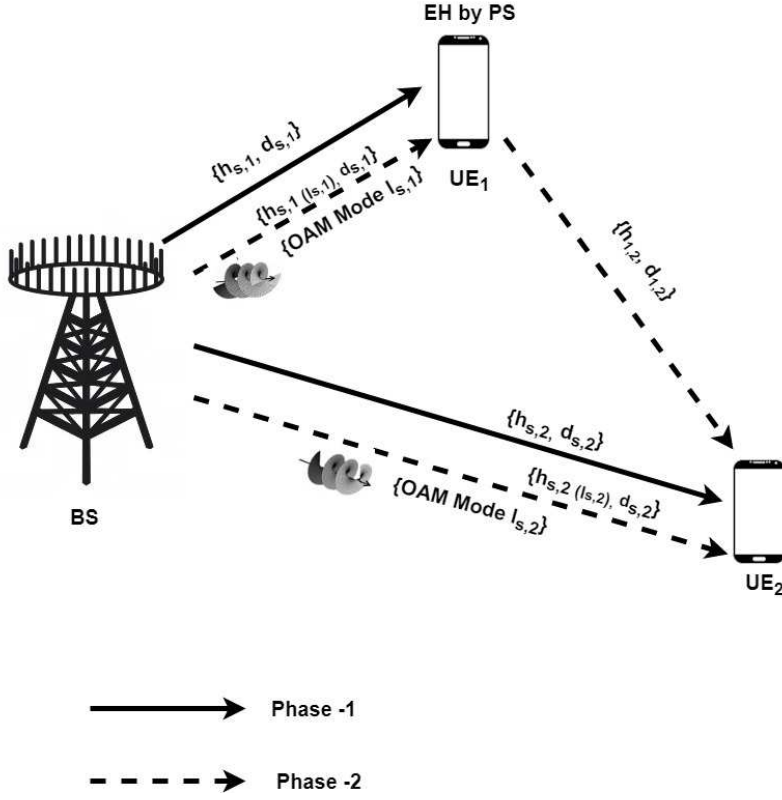


Fig. 1: Proposed system model for CNOMA-SWIPT-PS-OAM

2.1.1 Phase-1

Following the principle of downlink NOMA, BS transmits a superimposed composite signal $A = \sqrt{p_N}Px_1 + \sqrt{p_F}Px_2$ for a duration of $T/2$, where x_1, x_2 are the data symbols and p_N, p_F are power allocating factors respectively. Note that x_1, p_N and x_2, p_F are assigned to UE_1 and UE_2 , respectively. Moreover, the received power at UE_1 is split in the ratio of $\delta P : (1 - \delta)P$ ($0 \leq \delta \leq 1$), where δP and $(1 - \delta)P$ are for EH and information decoding (ID) respectively [22]. The transmitted power P_1 of UE_1 by harvested energy for DF relaying is given below

$$P_1 = \eta \delta P |h_{s,1}|^2. \quad (1)$$

Where, η is the energy conversion efficiency, where $0 \leq \eta \leq 1$ [14,18,22,24]. The received signals at UE_1 and UE_2 are respectively given by,

$$y_1 = (\sqrt{p_N(1 - \delta)P}x_1 + \sqrt{p_F(1 - \delta)P}x_2)|h_{s,1}|^2 + n_1, \quad (2)$$

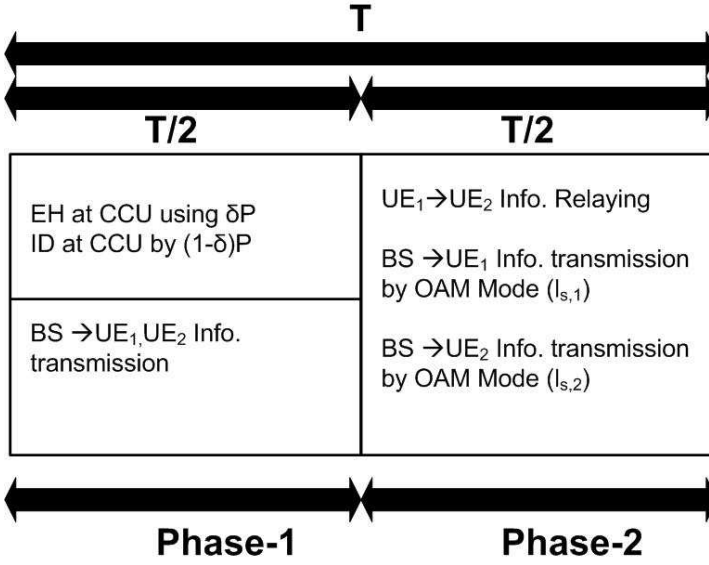


Fig. 2: Proposed protocol for CNOMA-SWIPT-PS-OAM

$$y_2 = (\sqrt{p_N(1-\delta)}x_1 + \sqrt{p_F(1-\delta)}x_2)|h_{s,2}|^2 + n_2, \quad (3)$$

where $n_1 \sim CN(0, \sigma^2)$ and $n_2 \sim CN(0, \sigma^2)$ are the complex AWGN at UE_1 and UE_2 respectively with zero mean and variance σ^2 . According to the downlink NOMA protocol, UE_1 first decodes x_2 and then performs SIC to decode own symbol x_1 [22]. Thus, the received SINR at UE_1 for x_2 and x_1 are respectively given by following equations

$$\gamma_{x_1}^{t_1} = (1-\delta)\rho|h_{s,1}|^2 p_N, \quad (4)$$

$$\gamma_{x_2 \rightarrow x_1}^{t_1} = \frac{(1-\delta)\rho|h_{s,1}|^2 p_F}{(1-\delta)\rho|h_{s,1}|^2 p_N + 1}, \quad (5)$$

where $\rho \triangleq \frac{P}{\sigma^2}$ is the transmit signal-to-noise ratio (SNR) by BS and $\gamma_{x_2 \rightarrow x_1}^{t_1}$ denotes the required SINR to decode symbol x_2 . Afterwards, UE_2 can obtain x_2 directly by treating x_1 as noise. Therefore the received SINR at UE_2 for x_2 can be derived by following equation

$$\gamma_{x_2}^{t_1} = \frac{\rho|h_{s,2}|^2(1-\delta)p_F}{\rho|h_{s,2}|^2(1-\delta)p_N + 1}. \quad (6)$$

Note that $p_N + p_F = 1 - \delta$ and $p_N < p_F$ [22].

2.1.2 Phase-2

This phase consists of cooperative DF relaying and BS transmits additional symbols to the UE_1 and UE_2 by different OAM modes to the users. The cooperative DF relay transmission from UE_1 to UE_2 and additional symbol transmission directly by different OAM modes from BS are performed on the remaining $T - T/2 = T/2$ duration. The cooperative relay is performed by UE_1 . UE_1 transmits the decoded symbol \hat{x}_2 to UE_2 by utilizing the harvested energy. The received signal at UE_2 by DF relaying is expressed below

$$\hat{y}_2 = \sqrt{P_1} \hat{x}_2 |h_{1,2}|^2 + n_2. \quad (7)$$

Therefore, the received SINR at UE_2 by DF relaying is obtained as below

$$\gamma_{x_2}^{t_2} = \rho \eta \delta |h_{s,1}|^2 |h_{1,2}|^2. \quad (8)$$

Two additional symbols x_3 for UE_1 and x_4 for UE_2 by using different LOS channels to UE_1 and UE_2 respectively from BS. BS transmit signal $B = \sqrt{P}x_3$ to UE_1 and signal $D = \sqrt{P}x_4$ to CEU for a duration of $T/2$ simultaneously. To mitigate the interference issue and effective transmission two different OAM modes $l_{s,1}$ and $l_{s,2}$ are considered for UE_1 and UE_2 respectively. The LOS channel coefficient $h_{y,z}(l_{y,z})$ between any two nodes y and $(y, z \in \{s, UE_1, UE_2\})$ and $y \neq z$ is subjected to LOS channel. The received signal at UE_1 and UE_2 from the BS by different OAM modes are given below

$$y_3 = (\sqrt{P}x_3) |h_{s,1,(l_{s,1})}|^2 + n_1. \quad (9)$$

$$y_4 = (\sqrt{P}x_4) |h_{s,2,(l_{s,2})}|^2 + n_2. \quad (10)$$

Accordingly, the received SINR for symbol x_3 at UE_1 can be expressed as [27-31]

$$\gamma_{x_3}^{t_2} = \rho \mu_1, \quad (11)$$

where μ_1 is the singular value of the channel response matrix $(h_{s,1,(l_{s,1})})$ of CNOMA-SWIPT-PS-OAM system [22,27,30]. OAM beam has divergence in its high-intensity region which caused attenuation [27-30]. By using Fresnel-zone-plate lenses antenna at BS, this issue can be mitigated without affecting the helical phase profile of OAM beam [27-30]. So, similarly the received SINR for symbol x_4 at UE_2 can be expressed as [29-31]

$$\gamma_{x_4}^{t_2} = \rho \mu_2, \quad (12)$$

where similarly as before μ_2 is the singular value of the channel response matrix $(h_{s,2,(l_{s,2})})$ of the proposed system [22,27,30].

2.2 Achievable capacity analysis

By considering normalized total time duration ($T = 1$). The equations for the capacities are derived in following segments.

2.2.1 Capacity of UE_1

x_1 and x_3 are received by UE_1 . So, the achievable capacity of UE_1 is obtained as below by (4) and (11),

$$C_{UE_1} = \frac{1}{2} \log_2(1 + \gamma_{x_1}^{t_1}) + \frac{1}{2} \log_2(1 + \gamma_{x_3}^{t_2}). \quad (13)$$

2.2.2 Capacity of UE_2

Using (5), (6), (8) and (12) the achievable capacity of UE_2 for x_2 and x_4 can be achieved by following equation,

$$C_{UE_2} = \frac{1}{2} \log_2(1 + \min(\gamma_{x_2 \rightarrow x_1}^{t_1}, \gamma_{x_2}^{t_1}, \gamma_{x_2}^{t_2})) + \frac{1}{2} \log_2(1 + \gamma_{x_4}^{t_2}). \quad (14)$$

2.2.3 Sum Capacity

So, the SC can be achieved by following equation [27]

$$C_{\text{sum}} = C_{UE_1} + C_{UE_2}. \quad (15)$$

Whereas, C_{UE_1} and C_{UE_2} are the capacity of UE_1 and UE_2 for the proposed CNOMA-SWIPT-PS-OAM technique.

2.3 Energy Efficiency of CNOMA-SWIPT-PS-OAM

Energy efficiency is the ratio of ergodic sum channel capacity (C_{sum}) and the total transmitted power by the BS for direct transmissions and transmission power from CCU for relaying. BS transmits P amount of power for direct transmissions for NOMA from BS. For additional symbol transmission by different OAM modes to the users from BS, P amount of power is also transmitted from BS as well. UE_1 transmit P_1 for DF relaying from UE_1 to UE_2 . So the EE can be derived as below for the proposed CNOMA-SWIPT-PS-OAM [34-35],

$$EE = \frac{C_{\text{sum}}}{2P + P_1}. \quad (16)$$

2.4 OMA-SWIPT-PS-OAM

For a fair comparison with the proposed CNOMA-SWIPT-PS-OAM scheme, OMA-SWIPT-PS-OAM scheme is also devised in this paper as benchmark. For the OMA case, time division multiple access (TDMA) is considered here. In this case, BS transmits information signal for UE_1 and UE_2 independently in different time slots with total transmit power P . The different time slots allocated for UE_1 and UE_2 for different symbols (e.g. x_1 , x_2 , x_3 and x_4) and DF relaying of x_2 are denoted as t_1 , t_2 , t_3 , and t_4 respectively. Moreover, PS

based SWIPT is considered at UE_1 [16,18,22]. Hence, UE_1 utilizes the fraction δ of the received power for energy harvesting and the remaining $1 - \delta$ fraction for ID [18,22,27]. So different transmission for x_1 , x_2 and DF relaying of x_2 utilizes single time slot for each transmission. Such as x_1 transmitted from BS to UE_1 in t_1 along with PS SWIPT based energy harvesting at UE_1 . x_2 is transmitting from BS to UE_2 in t_2 . Furthermore, DF relaying transmission of x_2 by utilizing the harvested energy from UE_1 to UE_2 is performed in t_3 . The transmission of x_3 and x_4 by different OAM modes ($l_{s,1}$ and $l_{s,2}$) are performed in t_4 . Because without interference by using different modes of OAM, different symbols can be transmitted to the users in same time slot (t_4). Moreover, since $T = 1$ is considered here, so total time slot is equally splitted for each time slot for OMA-SWIPT-PS-OAM technique. Hence, $t_1 = t_2 = t_3 = t_4 = \frac{1}{4}$ are considered here, which are the duration of each time slot. So, the achievable capacity of UE_1 and UE_2 can be achieved as below for the OMA-SWIPT-PS-OAM technique [5,27,33]

$$C_{UE_1}^{OMA} = \frac{1}{4} \log_2(1 + \rho(1 - \delta)|h_{s,1}|^2) + \frac{1}{4} \log_2(1 + \rho\mu_1). \quad (17)$$

$$C_{UE_2}^{OMA} = \frac{1}{4} \log_2(1 + \min(\rho(1 - \delta)|h_{s,2}|^2, \eta\delta\rho|h_{s,1}|^2|h_{1,2}|^2)) + \frac{1}{4} \log_2(1 + \rho\mu_2). \quad (18)$$

$$C_{\text{sum}}^{OMA} = C_{UE_1}^{OMA} + C_{UE_2}^{OMA}. \quad (19)$$

Moreover, $C_{UE_1}^{OMA}$ and C_{sum}^{OMA} are the capacity of CCU and CEU for OMA-SWIPT-PS-OAM technique. Moreover, EE can be derived as below for the OMA-SWIPT-PS-OAM [35-36],

$$EE_{OMA} = \frac{C_{\text{sum}}^{OMA}}{3P + P_1}. \quad (20)$$

So the above equation shows that EE is related to the C_{sum}^{OMA} , P and P_1 as before.

3 Numerical Results

In this section, results for the user capacities, SC and EE of the proposed protocol and techniques are examined and explained. The impact of changes in transmit SNR ρ , allowed power splitting factor δ , distance $d_{s,1}$ between BS and UE_1 on the performance of the considered system are discussed. Collinear placement of all nodes (e.g. BS, UE_1 , and UE_2) and normalized distances between any two nodes are considered, where $d_{s,1} = 0.5$, $d_{s,2} = 1$, and $d_{1,2} = 1 - d_{s,1}$. ($\Omega_{s,2} = 9$) < ($\Omega_{s,1} = \Omega_{1,2} = 36$) are considered for simulation [25,27]. Furthermore, normalized $P = 1$, normalized $T = 1$, $l_{s,1} = 2$ and $l_{s,2} = 1$ are considered here for simulation purpose. For performance

comparison, simulation results for CCU (UE_1) capacity, CEU (UE_2) capacity and SC of CNOMA-SWIPT-PS, CNOMA-SWIPT-TS, CNOMA-SWIPT-PS-OAM, and OMA-SWIPT-PS-OAM are also provided. Note that similar simulation parameters are considered for the proposed and other compared schemes for consistency.

3.1 User Capacities and Sum Capacity

The impact of ρ , $d_{s,1}$ and δ on the capacity of CCU, CEU, and SC of the proposed system is shown in this part. All figures are plotted for the parameters $K_{s,1} = K_{1,2} = 5$, and $K_{s,2} = 2$ due to Rician fading channel [25,27].

CCU (UE_1) capacity behavior with respect to (w.r.t) transmit SNR ρ is demonstrated in Figure 3 for the proposed CNOMA-SWIPT-PS-OAM scheme and compared with CNOMA-SWIPT-PS, CNOMA-SWIPT-TS, and OMA-SWIPT-PS-OAM schemes [22]. Parameters $p_N = 0.4$, $p_F = 0.6$, $\eta = 0.7$, $\delta = 0.3$, $d_{s,1} = 0.5$, $d_{s,2} = 1$, and $d_{1,2} = 1 - d_{s,1}$ are set during the simulation purpose. CCU capacity of all schemes increases linearly with an increase of ρ . CNOMA-SWIPT-PS-OAM exhibits far better performance than other schemes in case of CCU capacity because of additional symbol transmission from BS to CCU by an OAM mode ($l_{s,1}$). In the case of OMA-SWIPT-PS-OAM, CCU capacity is degraded than the proposed scheme due to using a dedicated time slot for each separate transmission from BS to CCU, excluding OAM based transmission.

Figure 4 represents CEU (UE_2) capacity behavior w.r.t transmit SNR ρ for the proposed CNOMA-SWIPT-PS-OAM and compared with CNOMA-SWIPT-PS, CNOMA-SWIPT-TS, and OMA-SWIPT-PS-OAM schemes as well. Parameters $p_N = 0.4$, $p_F = 0.6$, $\eta = 0.7$, $\delta = 0.3$, $d_{s,1} = 0.5$, $d_{s,2} = 1$, and $d_{1,2} = 1 - d_{s,1}$ are set during the simulation purpose as before. CEU capacity of all schemes increases linearly with increasing values of ρ . Figure 4 illustrates that in the case of CEU, the proposed scheme (CNOMA-SWIPT-PS-OAM) provides higher CEU capacity than other schemes as well. Similarly as before, an additional symbol is transmitting by utilizing the OAM beam with different OAM mode ($l_{s,2}$) on the time slot for relaying. Hence, the capacity is enhanced for the proposed technique at CEU. In the case of OMA-SWIPT-PS-OAM, CEU capacity is degraded than the proposed scheme due to using a dedicated time slot for each separate transmission from BS to CEU like as CCU, excluding OAM based transmission.

Figure 5 shows SC behavior w.r.t transmit SNR ρ for the proposed CNOMA-SWIPT-PS-OAM and compared with CNOMA-SWIPT-PS, CNOMA-SWIPT-TS, and OMA-SWIPT-PS-OAM schemes as well. Parameters $p_N = 0.4$, $p_F = 0.6$, $\eta = 0.7$, $\delta = 0.3$, $d_{s,1} = 0.5$, $d_{s,2} = 1$, and $d_{1,2} = 1 - d_{s,1}$ are set during the simulation purpose as before. Figure 5 illustrates that SC of all schemes increases linearly with the increasing values of ρ . Moreover, the proposed technique (CNOMA-SWIPT-PS-OAM) provides higher SC than other conventional techniques as well. The higher SC is achieved by utilizing the dif-

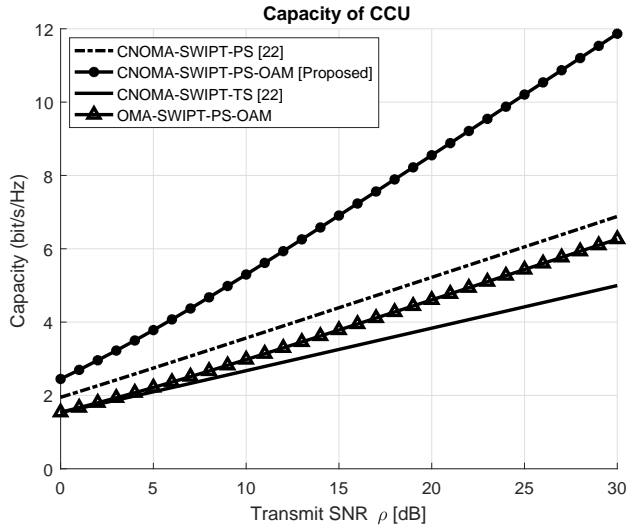


Fig. 3: Capacity comparisons of CCU with respect to transmit SNR ρ ; $K_{s,1} = K_{1,2} = 5$, $K_{s,2} = 2$, $p_N = 0.4$, $p_F = 0.6$, $P = 1$, $l_{s,1} = 2$, $l_{s,2} = 1$, $\delta = 0.3$, $\eta = 0.7$, $d_{s,1} = 0.5$ and $d_{s,2} = 1$.

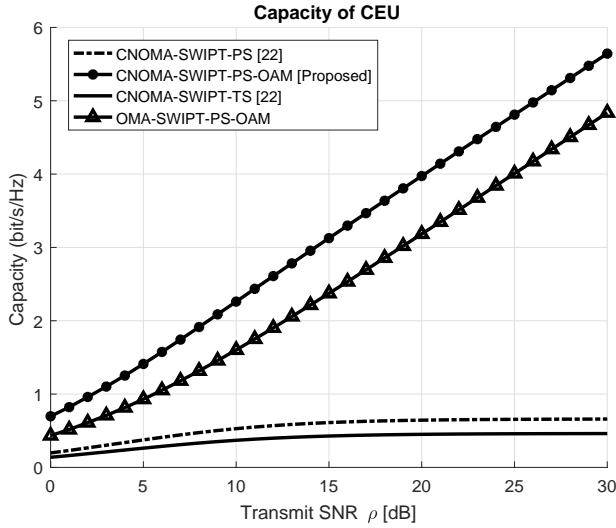


Fig. 4: Capacity comparisons of CEU with respect to transmit SNR ρ ; $K_{s,1} = K_{1,2} = 5$, $K_{s,2} = 2$, $p_N = 0.4$, $p_F = 0.6$, $P = 1$, $l_{s,1} = 2$, $l_{s,2} = 1$, $\delta = 0.3$, $\eta = 0.7$, $d_{s,1} = 0.5$ and $d_{s,2} = 1$.

ferent OAM modes to transmitting additional symbols to the CCU and CEU from the BS. Hence, the capacity of CCU and CEU for the proposed scheme

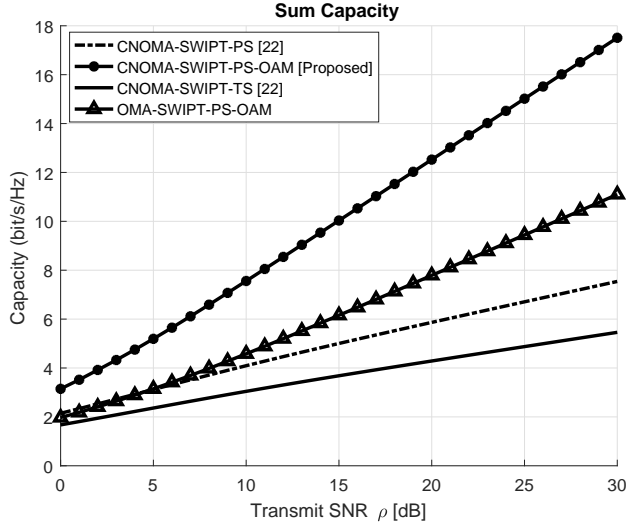


Fig. 5: SC comparisons with respect to transmit SNR ρ ; $K_{s,1} = K_{1,2} = 5$, $K_{s,2} = 2$, $p_N = 0.4$, $p_F = 0.6$, $P = 1$, $l_{s,1} = 2$, $l_{s,2} = 1$, $\delta = 0.3$, $\eta = 0.7$, $d_{s,1} = 0.5$ and $d_{s,2} = 1$.

are significantly higher than other existing schemes which is shown in Figure 3 and Figure 4. As a result, the SC of the proposed system is also enhanced significantly. In the case of OMA-SWIPT-PS-OAM, SC is lower than the proposed scheme because the capacities of CCU and CEU are comparatively lower than the proposed scheme (Which are shown in Figure 3 and Figure 4).

In Figure 6, the SC w.r.t $d_{s,1}$ is plotted for CNOMA-SWIPT-PS-OAM and compared with CNOMA-SWIPT-PS, CNOMA-SWIPT-TS, and OMA-SWIPT-PS-OAM schemes as well. Parameters $p_N = 0.4$, $p_F = 0.6$, $\eta = 0.7$, $\delta = 0.3$, and $\rho = 15dB$ are set during the simulation purpose. Figure 6 shows that due to increasing values of $d_{s,1}$, the SC is decreasing for all cases. This is happening because due to increasing values of $d_{s,1}$, the channel condition between BS and CCU is degraded. Moreover, p_N is lower than p_F as well due to NOMA [22]. So, CCU cannot decode the information properly due to the degradation of the channel from BS to CCU. Figure 6 also illustrates that due to the increase of $d_{s,1}$, the SC of the proposed scheme is comparatively higher than other conventional schemes. Due to the increasing values of $d_{s,1}$, the channel condition between BS to CCU is degrading as well. But due to the simultaneous transmission of additional symbols from BS to the users by different OAM modes is performed on the time duration of relaying. So, the achieved SC of the proposed scheme is significantly higher than other techniques due to the increasing values of $d_{s,1}$. Due to utilizing the separate time slot for each transmission, except OAM based transmission. So, the OMA-

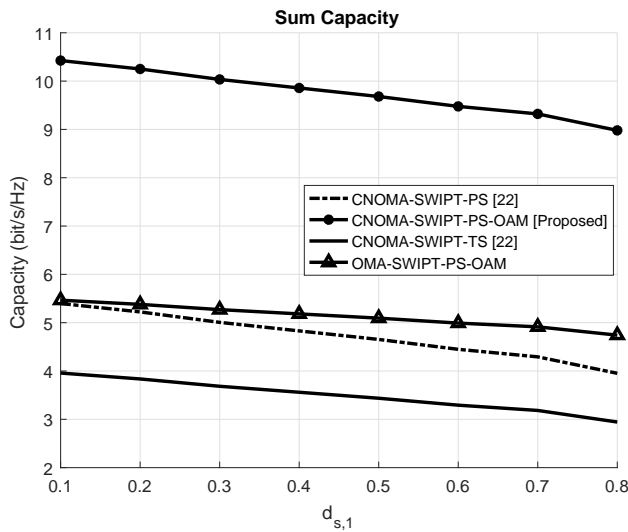


Fig. 6: SC comparisons with respect to $d_{s,1}$; $p_N = 0.4$, $p_F = 0.6$, $P = 1$, $l_{s,1} = 1$, $l_{s,2} = 2$, $\delta = 0.3$, $\eta = 0.7$ and $\rho = 15dB$.

SWIPT-PS-OAM scheme provides comparatively lower SC w.r.t $d_{s,1}$ than the proposed scheme which is illustrated in Figure 6 as well.

In Figure 7, the influence of δ over SC is plotted for CNOMA-SWIPT-PS-OAM and compared with CNOMA-SWIPT-PS, CNOMA-SWIPT-TS, and OMA-SWIPT-PS-OAM schemes as well. Parameters $p_N = 0.4$, $p_F = 0.6$, $\eta = 0.7$, $d_{s,1} = 0.5$, $d_{s,2} = 1$, $d_{1,2} = 1 - d_{s,1}$, and $\rho = 15dB$ are set during the simulation purpose. Figure 7 illustrates that due to increasing values of δ , the SC is decreasing for all schemes except CNMOMA-SWIPT-TS. Because in case of TS based SWIPT, there is no impact of δ [22]. Because δP is only used for energy harvesting for PS based SWIPT protocols. So, the higher values of δP can enhance the harvested energy for relaying. In contrast, the amount of harvested energy $((1 - \delta)P)$ for information decoding (ID) decreases as well for increasing values of δ . Hence, the information cannot decode properly at CCU. As a result, the SC is decreased for the increasing values of δ . Figure 7 shows that the proposed CNOMA-SWIPT-PS-OAM provides better SC than other schemes for different values of δ . Because the additional information transmission from BS to the users by different OAM modes can enhance the SC of the proposed scheme than other compared schemes significantly. Due to utilizing the separate time slot for each transmission except OAM based transmission, the OMA-SWIPT-PS-OAM scheme provides comparatively lower SC w.r.t δ than the proposed scheme which is illustrated in Figure 7 as before.

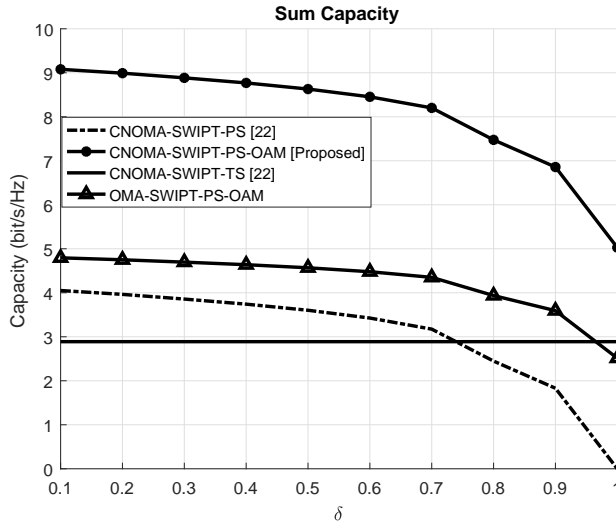


Fig. 7: SC comparisons with respect to δ ; $K_{s,1} = K_{s,2} = 5$, $K_{s,2} = 2$, $p_N = 0.4$, $p_F = 0.6$, $P = 1$, $l_{s,1} = 2$, $l_{s,2} = 1$, $\eta = 0.7$, $d_{s,1} = 0.5$, $d_{s,2} = 1$ and $\rho = 15dB$.

3.2 Energy Efficiency

EE shows the ratio of SC and total transmitted power. Impact of ρ , $d_{s,1}$ and δ on EE of the proposed scheme is shown in this part. All figures are plotted for the parameters $K_{s,1} = K_{1,2} = 5$, and $K_{s,2} = 2$ due to Rician fading channel [25,27].

EE w.r.t transmit SNR ρ is demonstrated in Figure 8 for the proposed CNOMA-SWIPT-PS-OAM and compared with CNOMA-SWIPT-PS, CNOMA-SWIPT-TS, and OMA-SWIPT-PS-OAM schemes [22]. Parameters $p_N = 0.4$, $p_F = 0.6$, $\eta = 0.7$, $\delta = 0.3$, $d_{s,1} = 0.5$, $d_{s,2} = 1$, and $d_{1,2} = 1 - d_{s,1}$ are set during the simulation purpose as before. The EE is going downwards due to the increasing number of transmit SNR ρ for every case. The transmitted power for relaying by the harvested energy is higher at CCU for higher values of ρ . That is why the EE is decreasing for higher ρ in all cases. Moreover, the proposed CNOMA-SWIPT-PS-OAM scheme provides higher EE than other schemes due to higher SC can be achieved by different OAM mode based transmission from BS to the users. So, Figure 8 illustrates that the proposed technique provides significantly higher EE than other conventional techniques as well. Because the SC is higher for the proposed CNOMA-SWIPT-PS-OAM technique than other compared schemes which is shown in Figure 5. Moreover, the PS based SWIPT provides higher EE than TS based SWIPT for CNOMA as well which is also shown in Figure 8 as well. Due to utilizing the separate time slot for each transmission except OAM based transmission, the OMA-

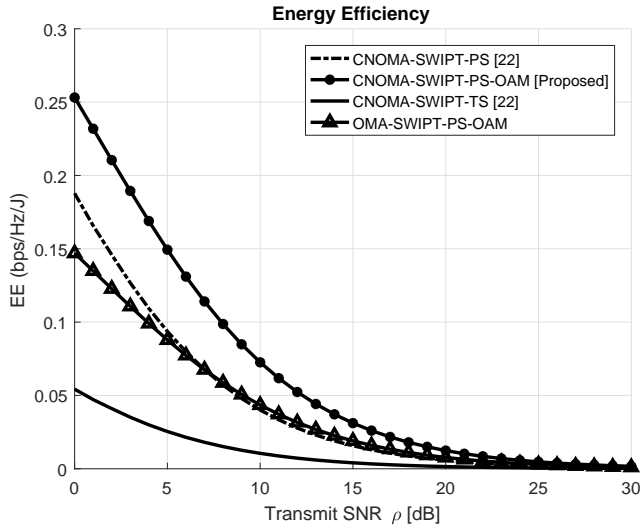


Fig. 8: EE comparisons with respect to transmit SNR ρ ; $K_{s,1} = K_{1,2} = 5$, $K_{s,2} = 2$, $p_N = 0.4$, $p_F = 0.6$, $P = 1$, $l_{s,1} = 2$, $l_{s,2} = 1$, $\delta = 0.3$, $\eta = 0.7$, $d_{s,1} = 0.5$ and $d_{s,2} = 1$.

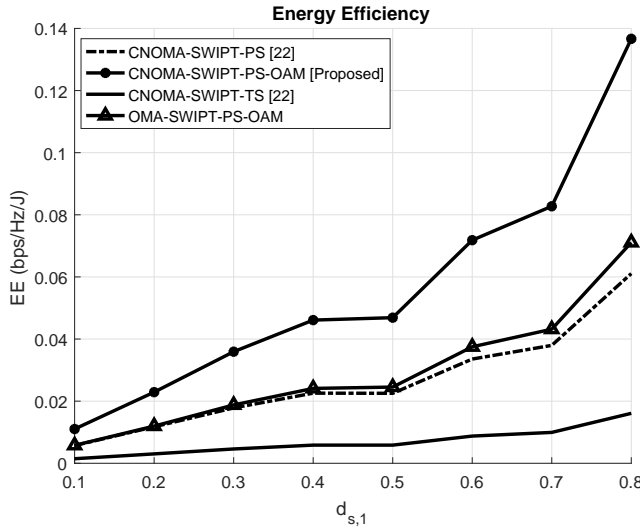


Fig. 9: EE comparisons with respect to $d_{s,1}$; $p_N = 0.4$, $p_F = 0.6$, $P = 1$, $l_{s,1} = 1$, $l_{s,2} = 2$, $\delta = 0.3$, $\eta = 0.7$ and $\rho = 15dB$.

SWIPT-PS-OAM scheme provides comparatively lower EE than the proposed scheme w.r.t ρ which is illustrated in Figure 8.

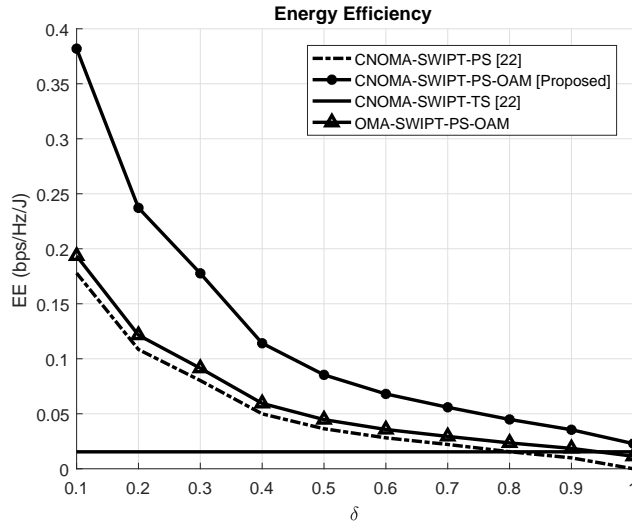


Fig. 10: EE comparisons with respect to δ ; $K_{s,1} = K_{s,2} = 5$, $K_{s,2} = 2$, $p_N = 0.4$, $p_F = 0.6$, $P = 1$, $l_{s,1} = 2$, $l_{s,2} = 1$, $\eta = 0.7$, $d_{s,1} = 0.5$, $d_{s,2} = 1$ and $\rho = 15dB$.

In Figure 9, the EE w.r.t $d_{s,1}$ is plotted for CNOMA-SWIPT-PS-OAM and compared with CNOMA-SWIPT-PS, CNOMA-SWIPT-TS, and OMA-SWIPT-PS-OAM schemes as well. Parameters $p_N = 0.4$, $p_F = 0.6$, $\eta = 0.7$, $\delta = 0.3$, and $\rho = 15dB$ are set during the simulation purpose. The EE is increasing for all cases in Figure 9. This happens because of the increasing value of $d_{s,1}$ causes a reduction of transmit power for relaying (P_1) at CCU due to degradation of channel conditions between BS and CCU. The EE is significantly higher for the proposed CNOMA-SWIPT-PS-OAM scheme than other schemes which is shown in Figure 9. Because according to Figure 6, the SC of the proposed scheme is significantly higher than other schemes due to additional symbol transmission from BS to the users by different OAM modes. Due to utilizing the separate time slot for each transmission except OAM based transmission, the OMA-SWIPT-PS-OAM scheme provides significantly lower EE than the proposed scheme w.r.t $d_{s,1}$ which is illustrated in Figure 9.

In Figure 10, the impact of δ over EE is plotted for CNOMA-SWIPT-PS-OAM and compared with CNOMA-SWIPT-PS, CNOMA-SWIPT-TS, and OMA-SWIPT-PS-OAM schemes as well. Parameters $p_N = 0.4$, $p_F = 0.6$, $\eta = 0.7$, $d_{s,1} = 0.5$, $d_{s,2} = 1$, $d_{1,2} = 1 - d_{s,1}$, and $\rho = 15dB$ are set during the simulation purpose. The EE is decreasing for increasing value of δ . According to Figure 7, SC is decreasing for increasing values of δ . Moreover, Figure 7 shows that the proposed CNOMA-SWIPT-PS-OAM provides better SC than other schemes for different values of δ as well. The additional information transmission by different OAM modes boosts up the SC of the proposed scheme

than other schemes significantly. As a result, the EE is higher for the proposed scheme than other schemes which is shown in Figure 10. In addition, there is no impact of δ on SC of CNMOMA-SWIPT-TS. Because δ is only used for energy harvesting for PS based SWIPT protocols [22]. So there is no impact of δ on EE of CNMOMA-SWIPT-TS scheme as well. Due to utilizing the separate time slot for each transmission except OAM based transmission, the OMA-SWIPT-PS-OAM scheme provides significantly lower EE than the proposed scheme w.r.t δ which is illustrated in Figure 10.

4 Conclusion

In this paper, the CNOMA-SWIPT-PS-OAM scheme has been proposed to enhance the capacities and energy efficiency of PS SWIPT based CNOMA downlink transmission. Moreover, OMA-SWIPT-PS-OAM and other two conventional schemes such as CNOMA-SWIPT-PS and CNOMA-SWIPT-TS are also compared with the proposed scheme for a fair comparison. According to result analysis, it is shown that the proposed scheme provides better performance compared to other conventional schemes in terms of capacities and energy efficiency. In the future, the work can be extended by incorporating amplify and forward relay assisted CNOMA with the proposed scheme.

Acknowledgements This work was supported by the National Research Foundation of Korea(NRF) grant funded by the Korea government(MEST) (No. 2019R1A2C1089542)

References

1. DoCoMo NTT. "5G Radio Access: Requirements, Concept and Technologies", White Paper, (2014).
2. Yazaki, Takahiro, and Yukitoshi Sanada. Effect of Joint Detection in Far User on Non-Orthogonal Multiple Access Downlink. *Wireless Personal Communications*, 89, no. 4, 120319, (2016).
3. Razavi, Razieh, Mehrdad Dianati, and Muhammad Ali Imran. Non-Orthogonal Multiple Access (NOMA) for Future Radio Access. *5G Mobile Communications*, 13563, (2016).
4. Dai, Linglong, Bichai Wang, Yifei Yuan, Shuangfeng Han, Chih-Lin I, and Zhaocheng Wang. Non-Orthogonal Multiple Access for 5G: Solutions, Challenges, Opportunities, and Future Research Trends. *IEEE Communications Magazine* 53, no. 9, 7481, (2015).
5. Kader, Md. Fazlul, Soo Young Shin, and Victor C. M. Leung. Full-Duplex Non-Orthogonal Multiple Access in Cooperative Relay Sharing for 5G Systems. *IEEE Transactions on Vehicular Technology* 67, no. 7, (2018).
6. Zhang, Yangyang, Jianhua Ge, and Erchin Serpedin. On the Performance of a Nonorthogonal Multiple-Access Technique for Downlink MIMO Cooperative Networks., *Transactions on Emerging Telecommunications Technologies* 29, no. 1, (2017).
7. Kim, Jung-Bin, and In-Ho Lee. Non-Orthogonal Multiple Access in Coordinated Direct and Relay Transmission, *IEEE Communications Letters* 19, no. 11, 203740, (2015).
8. Kader, Md. Fazlul, and Soo Young Shin. Cooperative Relaying Using Space-Time Block Coded Non-Orthogonal Multiple Access. *IEEE Transactions on Vehicular Technology*, 66, no. 7, 58945903, (2017).
9. Kader, Md. Fazlul, Muhammad Basit Shahab, and Soo Young Shin. Exploiting Non-Orthogonal Multiple Access in Cooperative Relay Sharing. *IEEE Communications Letters*, 21, no. 5, 115962, (2017).

10. Atallah, Ribal, Maurice Khabbaz, and Chadi Assi. Energy Harvesting in Vehicular Networks: a Contemporary Survey, *IEEE Wireless Communications*, 23, no. 2, 7077, (2016).
11. Yan, Jia, and Yuan Liu. A Dynamic SWIPT Approach for Cooperative Cognitive Radio Networks, *IEEE Transactions on Vehicular Technology*, 66, no. 12, 1112236, (2017).
12. Varshney, Lav R. Transporting Information and Energy Simultaneously, *IEEE International Symposium on Information Theory*, (2008).
13. Nasir, Ali A., Xiangyun Zhou, Salman Durrani, and Rodney A. Kennedy. Relaying Protocols for Wireless Energy Harvesting and Information Processing, *IEEE Transactions on Wireless Communications*, 12, no. 7, 362236, (2013).
14. Do TN, da Costa DB, Duong TQ, An B. "Improving the performance of celledge users in MISONOMA systems using TAS and SWIPTbased cooperative transmissions.", *IEEE Trans Green Commun Network*, 2, no. 1, 4962, (2018).
15. Do, Nhu Tri, Daniel Benevides Da Costa, Trung Q. Duong, and Beongku An. A BNBf User Selection Scheme for NOMA-Based Cooperative Relaying Systems With SWIPT. *IEEE Communications Letters*, 21, no. 3, (2017) .
16. Ye, Yinghui, Yongzhao Li, Dan Wang, and Guangyue Lu. Power Splitting Protocol Design for the Cooperative NOMA with SWIPT. 2017 IEEE International Conference on Communications (ICC), (2017).
17. Liu, Yuanwei, Zhiguo Ding, Maged ElKashlan, and H. Vincent Poor. Cooperative Non-Orthogonal Multiple Access With Simultaneous Wireless Information and Power Transfer. *IEEE Journal on Selected Areas in Communications* 34, no. 4, 93853, (2016).
18. Amin, Ahmed Al, and Soo Young Shin. Investigate the Dominating Factor of Hybrid SWIPT Protocol by Performance Analysis of the Far User of Hybrid SWIPT Based CNOMA Downlink Transmission. 2019 International Conference on Electrical, Computer and Communication Engineering (ECCE), (2019).
19. Kader MF, Shahab MB, Shin SY. "Cooperative spectrum sharing with energy harvesting best secondary user selection and nonorthogonal multiple access", 2017 International Conference on Computing, Networking and Communications (ICNC); Santa Clara, CA, USA, (2017).
20. Yang Z, Ding Z, Fan P, Aldhahir N. The impact of power allocation on cooperative nonorthogonal multiple access networks with SWIPT. *IEEE Trans Wirel Communication*, 16, no.7, 43324343, (2017).
21. Diamantoulakis, Panagiotis D., Koralia N. Pappi, Zhiguo Ding, and George K. Karagiannidis. Wireless-Powered Communications With Non-Orthogonal Multiple Access. *IEEE Transactions on Wireless Communications* 15, no. 12, 842236, (2016).
22. Kader, Md. Fazlul, Mohammed Belal Uddin, Anik Islam, and Soo Young Shin. Cooperative NonOrthogonal Multiple Access with SWIPT over Nakagami m Fading Channels. *Transactions on Emerging Telecommunications Technologies*, 30, no. 5 (2019).
23. Shah, Syed Tariq, Kae Won Choi, Tae-Jin Lee, and Min Young Chung. Outage Probability and Throughput Analysis of SWIPT Enabled Cognitive Relay Network With Ambient Backscatter. *IEEE Internet of Things Journal* 5, no. 4, 31983208, (2018).
24. Do, Nhu Tri, Daniel Benevides Da Costa, Trung Q. Duong, and Beongku An. Transmit Antenna Selection Schemes for MISO-NOMA Cooperative Downlink Transmissions with Hybrid SWIPT Protocol. 2017 IEEE International Conference on Communications (ICC), France, (2017).
25. Jiao, R., Dai, L., Zhang, J., Mackenzie, R., and Hao, M., "On the Performance of NOMA-Based Cooperative Relaying Systems Over Rician Fading Channels", *IEEE Transactions on Vehicular Technology*, 66, no.12, 11409-11413, (2017).
26. Wang, L., Ge, X., Zi, R., and Wang, C., "Capacity Analysis of Orbital Angular Momentum Wireless Channels", *IEEE Access*, no.5, 23069-23077, (2017).
27. Amin A.A., Narottama, B., Shin S.Y. "Capacity Enhancement of Cooperative NOMA over Rician Fading Channels with Orbital Angular Momentum", arXiv:1906.09026 [eess.SP].
28. Basar, Ertugrul. Orbital Angular Momentum With Index Modulation. *IEEE Transactions on Wireless Communications* 17, no. 3, 202937, (2018).
29. Gao, Xinlu, Shanguo Huang, Yongfeng Wei, Wensheng Zhai, Wenjing Xu, Shan Yin, Jing Zhou, and Wanyi Gu. An Orbital Angular Momentum Radio Communication System Optimized by Intensity Controlled Masks Effectively: Theoretical Design and Experimental Verification. *Applied Physics Letters* 105, no. 24 , 241109, (2014).

-
30. Wang, Lei, Fa Jiang, Zhe Yuan, Jie Yang, Guan Gui, and Hikmet Sari. Mode Division Multiple Access: a New Scheme Based on Orbital Angular Momentum in Millimetre Wave Communications for Fifth Generation. *IET Communications*, no. 12, 141621, (2018).
 31. Saito, Yuya, Anass Benjebbour, Yoshihisa Kishiyama, and Takehiro Nakamura. System-Level Performance Evaluation of Downlink Non-Orthogonal Multiple Access (NOMA). 2013 IEEE 24th Annual International Symposium on Personal, Indoor, and Mobile Radio Communications (PIMRC), (2013).
 32. Ge, Xiaohu, Ran Zi, Xusheng Xiong, Qiang Li, and Liang Wang, Millimeter Wave Communications With OAM-SM Scheme for Future Mobile Networks. *IEEE Journal on Selected Areas in Communications* 35, no. 9, 216377, (2017).
 33. Kader, Md. Fazlul, and Soo Young Shin. Coordinated Direct and Relay Transmission Using Uplink NOMA, *IEEE Wireless Communications Letters* 7, no. 3, 400403, (2018).
 34. Cheng, Wenchi, Wei Zhang, Haiyue Jing, Shanghua Gao, and Hailin Zhang. Orbital Angular Momentum for Wireless Communications, *IEEE Wireless Communications* 26, no. 1, 100107, (2019).
 35. Huang, Yuwen, Mengyu Liu, and Yuan Liu. Energy-Efficient SWIPT in IoT Distributed Antenna Systems, *IEEE Internet of Things Journal* 5, no. 4, 264656, (2018).
 36. Amin A.A., Uddin, M.B., Shin S.Y., "Performance Enhancement of Hybrid SWIPT Protocol for Cooperative NOMA Downlink Transmission", arXiv:1906.09159 [eess.SP].